

Observing the origin of superconductivity in quantum critical metals

J.-H. She, B. J. Overbosch, Y.-W. Sun, Y. Liu, K. E. Schalm, J. A. Mydosh, and J. Zaanen

Instituut-Lorentz for Theoretical Physics, Universiteit Leiden,

P. O. Box 9506, 2300 R A Leiden, The Netherlands

(Dated: September 26, 2018 [file: pairTunPRB-JHS2])

Despite intense efforts during the last 25 years, the physics of unconventional superconductors, including the cuprates with a very high transition temperature, is still a controversial subject. It is believed that superconductivity in many of these strongly correlated metallic systems originates in the physics of quantum phase transitions, but quite diverse perspectives have emerged on the fundamentals of the electron-pairing physics, ranging from Hertz style critical spin fluctuation glue to the holographic superconductivity of string theory. Here we demonstrate that the gross energy scaling differences that are behind these various pairing mechanisms are directly encoded in the frequency and temperature dependence of the dynamical pair susceptibility. This quantity can be measured directly via the second order Josephson effect and it should be possible employing modern experimental techniques to build a ‘pairing telescope’ that gives a direct view on the origin of quantum critical superconductivity.

I. INTRODUCTION AND SUMMARY

The large variety of superconductors that are not explained by the classic Bardeen-Cooper-Schrieffer (BCS) theory include the cuprates^{1,2} and iron pnictides³ with their (very) high transition temperatures (T_c ’s), but also the large family of low T_c heavy fermion superconductors.^{1,4} These materials have in common that the dominance of electronic repulsions create an environment that is *a priori* very unfavorable for conventional superconductivity. Their unconventional (non-*s*-wave) order parameters indeed signal that dissimilar physics is at work. Based on a multitude of experiments, a widely held hypothesis has arisen that the physics of many of these systems is controlled by a quantum phase transition.^{5–8} This would generate a scale invariant quantum physics in the electron system, as it does for any other second order phase transition, and the imprint of this universal critical behavior on the metallic state creates the conditions for unconventional superconductivity.

We propose to test this hypothesis of quantum-criticality as the fundamental physics underlying the onset of superconductivity directly. A clean probe can be identified: a measurement of the dynamical order-parameter susceptibility — the Cooper pair susceptibility — of the quantum critical superconductor in its normal state in a large temperature and energy interval. Four differing theoretical views of electron-quantum-criticality that are available — including two brand new paradigms descending from string theory — all allow for explicit computations of the susceptibility.^{9–12} At the same time, the pair susceptibility can be measured directly via the so-called second order Josephson effect in superconductor-insulator-superconductor (SIS) junctions involving superconductors with different transition temperatures.^{13,14}

Goldman and collaborators delivered proof of principle in the 1970s by measuring the pair susceptibility in the normal state of aluminum in an aluminum-aluminum oxide-lead junction.^{15,16} In this experiment the order parameter of the “strong” superconductor with a “high” T_c^{high} acts as an external perturbing field on the metallic electron system realized above the transition of the superconductor with a much lower T_c^{low} . In the temperature regime $T_c^{\text{low}} \leq T \ll T_c^{\text{high}}$ and for an applied bias eV less than the gap Δ_{high} of the strong superconductor the current through a tunneling junction between the two is directly proportional to the imaginary part of the dynamical pair susceptibility. This higher order Cooper pair tunneling process is a second order Josephson effect: if at low temperatures the regular dc Josephson effect can be observed (i.e., a finite supercurrent at zero bias in SIS configuration), then the higher order tunneling Cooper pair process is likely to occur in the superconductor-insulator-normal-state (SIN) configuration at finite bias.

Quite recently Bergeal et al.¹⁷ succeeded to get a signal on a 60 K underdoped cuprate superconductor using a 90 K cuprate source. This was motivated by the prediction that an asymmetric relaxational peak would be found signaling the dominance of phase fluctuations in the order parameter dynamics of the underdoped cuprate.¹⁸ Although this prediction was not borne out by the experiment it is for the present purposes quite significant that Bergeal et al. managed to isolate the second order Josephson current at such a high temperature (60 K) in *d*-wave superconductors where the masking effects of the quasiparticle currents should be particularly severe. As we will explain from our theoretical predictions, the unambiguous information regarding the quantum critical pairing mechanism resides in the large dynamical range in temperature and frequency of the pair susceptibility meaning that in principle one should measure up to temperatures of order $50 \times T_c$ and energies greater than ten times the gap of the weak superconductor (we set $T_c^{\text{low}} = T_c$ from here on). The system that is interrogated should therefore be a quantum critical system with a low T_c and the natural candidates are heavy fermion superconductors characterized by quantum critical points at

ambient conditions. We shall propose two explicit experimental approaches using modern thin film techniques and STM/STS/PCS techniques with a superconducting tip to obtain the pair-susceptibility in the range of temperature and frequency that will distinguish between the differing quantum-critical metal models.

Theoretically the pair susceptibility is defined as

$$\chi_p(\mathbf{q}, \omega) = -i \int_0^\infty dt e^{i\omega t - 0^+ t} \langle [b^\dagger(\mathbf{q}, 0), b(\mathbf{q}, t)] \rangle, \quad (1)$$

where the Cooper pair order parameter $b^\dagger(\mathbf{q}, t)$ is built out of the usual annihilation (creation) operators for electrons $c_{\mathbf{k}, \sigma}^{(\dagger)}$ with momentum \mathbf{k} and spin σ . In the s -channel $b^\dagger(\mathbf{q}, t) = \sum_{\mathbf{k}} c_{\mathbf{k}+\mathbf{q}/2, \uparrow}^\dagger(t) c_{-\mathbf{k}+\mathbf{q}/2, \downarrow}^\dagger(t)$. The imaginary (absorptive) part of this susceptibility at zero-momentum is measured by the second order Josephson effect. In figure 1 we show the theoretical results for standard BCS theory compared to four different limiting scenarios for the quantum critical metallic state. This is our main result: the contrast is discernable by the naked eye and this motivates our claim that this is an excellent probe of the fundamental physics underlying the onset of superconductivity. We will make clear that the specific temperature evolution of the dynamical pair susceptibility directly reflects the distinct RG flows underlying the superconducting instability in each case.

In detail the five types (A-E) of pairing mechanisms whose susceptibility is given in Fig. 1 are:

Case A is based upon traditional Fermi liquid BCS theory and is included for comparison. The dynamical pair susceptibility is calculated through an Eliashberg-type computation assuming a conventional Fermi-liquid interacting with “glue bosons” in the form of a single-frequency oscillator.^{19–21} Such a pair susceptibility would be found when the superconductivity would be due to “superglue” formed by bosons with a rather well defined energy scale as envisaged in some spin fluctuation scenarios.^{22,23}

Case B reflects the main stream thinking in condensed matter physics. It rests on the early work of Hertz²⁴ and asserts that the essence of BCS theory is still at work, i.e., one can view the normal state at least in a perturbative sense as a Fermi-liquid, which coexists with a bosonic order parameter field undergoing the quantum phase transition. The order parameter itself is Landau damped by the particle-hole excitations, while the quantum critical fluctuations in turn couple strongly to the quasiparticles explaining the anomalous properties of the metallic state.⁶ Eventually the critical bosons cause the attractive interactions driving the pairing instability.²⁵ This notion is coincident with the idea that the pairing is due to spin fluctuations when the quantum phase transition involves magnetic order (as in the heavy fermions and pnictides) while in the cuprate community a debate rages at present concerning the role of other “pseudogap” orders like spontaneous currents and quantum nematics. The computation of the pair-susceptibility amounts to solving the full Eliashberg equations for a glue function that itself is algebraic in frequency $\lambda(\omega) \sim 1/\omega^\gamma$ in the strong coupling regime as formulated by Chubukov and coworkers.^{9,26,27} At first sight the resulting Fig. 1 B looks similar to the remaining cases C-E that contain more radical assumptions regarding the influence of the quantum scale invariance. However, as we will see, case B should leave a strong fingerprint in the data in the form of a strong violation of energy-temperature scaling (Fig. 2B).

Case C is a simple phenomenological “quantum critical BCS” scaling theory.¹⁰ It is like BCS in the sense that a simple pairing glue is invoked but now it is assumed that the normal state is a non-Fermi liquid which is controlled by conformal invariance. In other words, the ‘bare’ pair propagator $\chi_{\text{pair}}^0(\omega, T)$, in the absence of glue, is described by a scaling function. The full pair susceptibility is then given by the RPA expression

$$\chi_{\text{pair}}(\omega, T) = \frac{\chi_{\text{pair}}^0(\omega, T)}{1 - V \chi_{\text{pair}}^0(\omega, T)}, \quad (2)$$

where V is the effective attractive interaction, that is non-retarded for simplicity. The pairing instability occurs when $1 - V[\chi_{\text{pair}}^0(\omega = 0, T_c)]' = 0$. In quantum critical BCS one takes $\chi_{\text{QBCS}}^0(\omega) \sim 1/(i\omega)^\delta$, valid when $\omega \gg T$, as opposed to standard BCS where the bare fermion loop of the Fermi-gas yields a “marginal” pair propagator $\chi_{\text{BCS}}^0(\omega) = (1/E_F)[\log(\omega/E_F) + i]$. One can now deform the “marginal” Fermi liquid BCS case $\delta = 0$ to “relevant” pairing operators, i.e., with scaling exponent $\delta > 0$. One effect of this power-law scaling is that T_c becomes much larger. Our full calculations include finite temperature effects which serves as an IR cut-off and incorporate a retarded nature of the interaction by considering an Eliashberg-style generalization of equation (2). Such power-law scaling behavior was recently identified in numerical dynamical cluster approximation calculations on the Hubbard model.²⁸ This was explained in terms of a marginal Fermi liquid (MFL), i.e. the electron scattering rate proportional to the larger of temperature or frequency, in combination with a band structure characterized by a van Hove singularity (vHS) which is precisely located at the Fermi energy.²⁹ The vHS is essential; a MFL self-energy added to standard BCS or critical glue alone will not produce the power-law scaling. The presence of a vHS can be measured independently by ARPES^{30,31} and tunneling spectroscopy³² and therefore all the information is available in principle to distinguish this particular mechanism from the other cases. A careful study of the MFL pair susceptibility with both a smooth density of states and vHS is included in Appendix B.

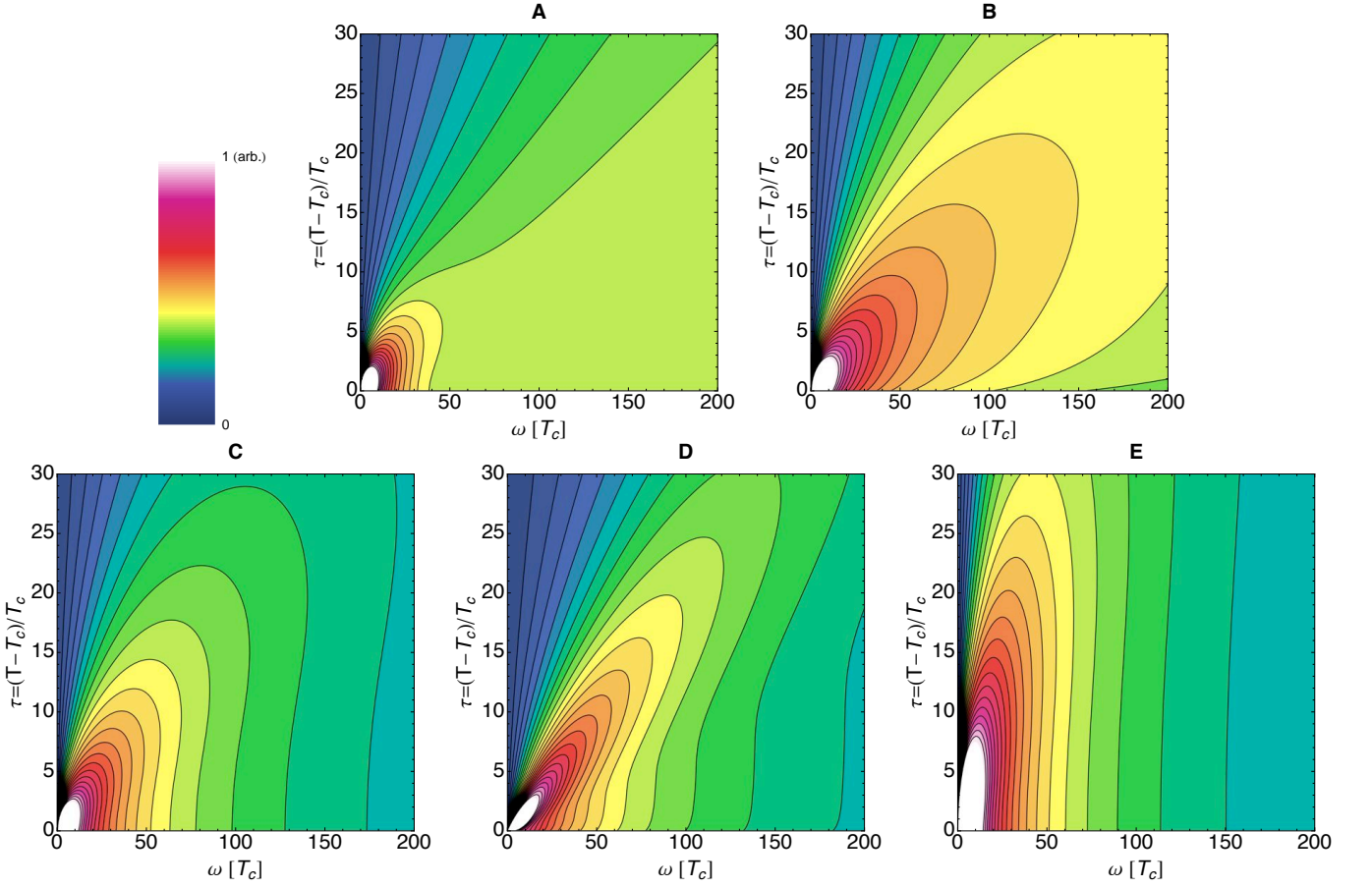


FIG. 1: (Color online) **Imaginary part of the pair susceptibility.** **A-E**, False-color plot of the imaginary part of the pair susceptibility $\chi''(\omega, T)$ in arbitrary units as function of ω (in units of T_c) and reduced temperature $\tau = (T - T_c)/T_c$, for five different cases: case A represents the traditional Fermi liquid BCS theory (see section III case A with parameters $T_c = 0.01$, $g \approx 0.39$, $\omega_b = 0.45$), case B is the Hertz-Millis type model with a critical glue (see section III case B with parameters $\gamma = \frac{1}{3}$, $T_c = 0.01$, $\Omega_0 \approx 0.0027$), case C is the phenomenological “quantum critical BCS” theory (see section III case C with $\delta = \frac{1}{2}$, $T_c = 0.01$, $g \approx 0.19$, $\omega_b \approx 0.1$, $x_0 = 2.665$), case D corresponds to the “large charge” holographic superconductor with AdS_4 type scaling (see section III case D with $\delta = \frac{1}{2}$, $T_c \approx 0.40$, $e = 5$) and case E is the “small charge” holographic superconductor with an emergent AdS_2 type scaling (see section III case E with $\delta = \frac{1}{2}$, $T_c \approx 1.4 \times 10^{-10}$, $e \approx 0$, $g = -\frac{17}{96}$, $\kappa \approx -0.36$). $\chi''(\omega, T)$ should be directly proportional to the measured second order Josephson current (experiment discussed in the text). In the bottom left of each plot is the relaxational peak that diverges (white colored regions are off-scale) as T approaches T_c . This relaxational peak looks qualitatively quite similar for all five cases, while only at larger temperatures and frequencies qualitative differences between the five cases become manifest.

Cases D and E are radical departures of established approaches to superconductivity that emerged very recently from string theory. They are based on the anti-de-Sitter/conformal field theory correspondence (AdS/CFT) or “holographic duality”,^{33–35} asserting that the physics of extremely strongly interacting quantum critical matter can be encoded in quasi-classical gravitational physics in a space-time with one more dimension. Including a charged black-hole in the center, a finite temperature and density is imposed in the field theory, and the fermionic response of the resulting state is remarkably suggestive of the strange-metal behavior seen experimentally in quantum critical metals. Although the (large- N super-Yang-Mills) field theories that AdS/CFT can explicitly address are remote to the physics of electrons in solids, there is much evidence suggesting that the correspondence describes generic “scaling histories”. AdS/CFT can be viewed as a generalization of the Wilson-Fisher renormalization group that handles deeply-non-classical many-particle entanglements, for which the structure of the renormalization flow is captured in the strongly constrained gravitational physics of the holographic dual. As such holography provides a new mechanism for superconductivity: it requires, gravitationally encoded in black hole superradiance, that the finite density quantum critical metal turns into a superconducting state when temperature is lowered.^{11,36} This holographic superconductivity (HS) is “without glue”: HS is an automatism wired in the renormalization flow originating in the extreme thermodynamical instability of the uncondensed quantum critical metal at zero temperature. As we illustrate in Fig. 1, AdS/CFT provides fundamentally

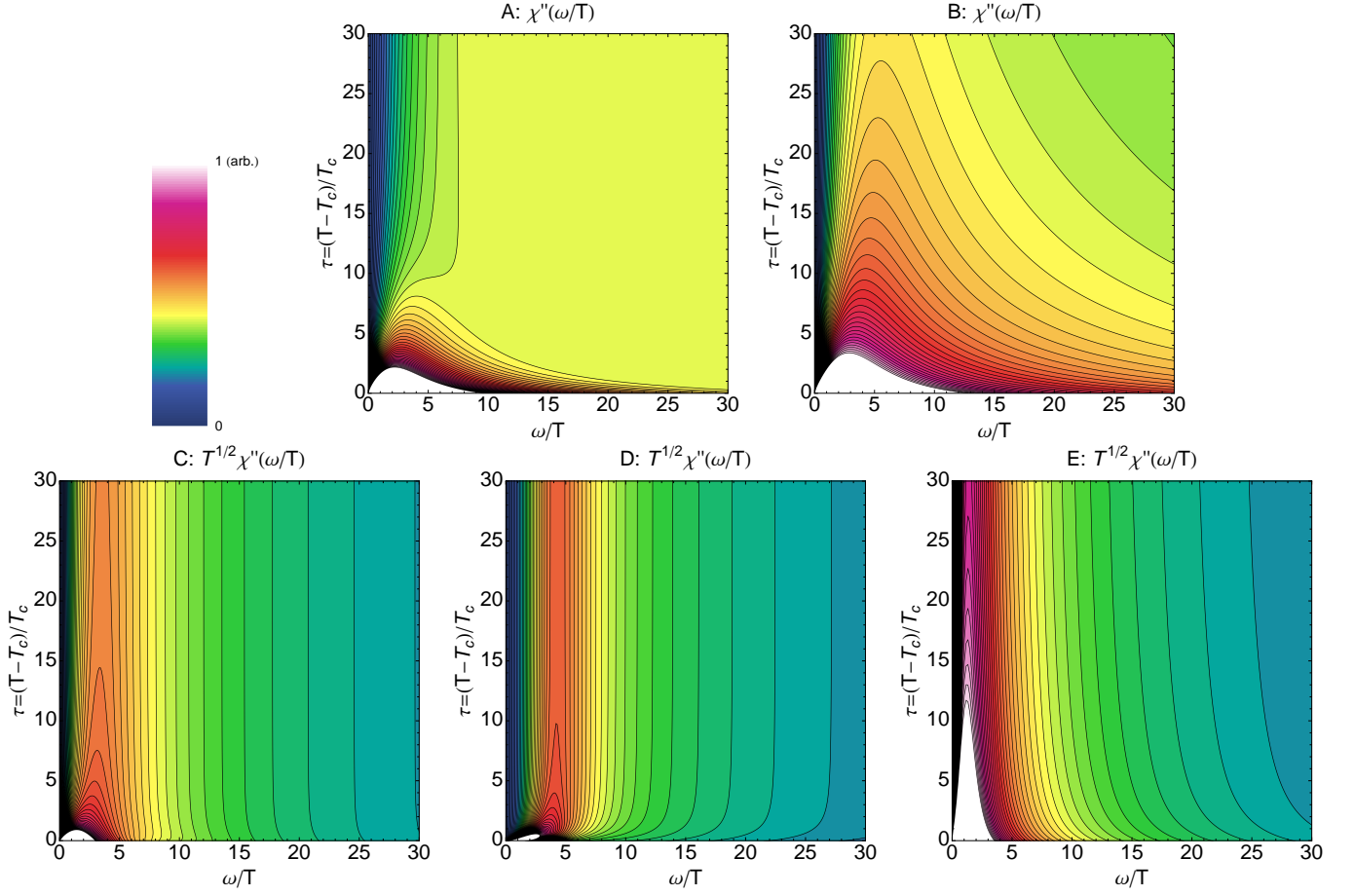


FIG. 2: (Color online) **Energy-temperature scaling of the pair susceptibility.** A-E, False-color plots of the imaginary part of the pair susceptibility, like in Fig. 1, but now the horizontal axis is rescaled by temperature while the magnitude is rescaled by temperature to a certain power: we are plotting $T^\delta \chi''(\omega/T, \tau)$, in order to show energy-temperature scaling at high temperatures. For quantum critical BCS (case C), AdS₄ (case D) and AdS₂ (case E), with a suitable choice of the exponent $\delta > 0$, the contour lines run vertically at high temperatures, meaning that the imaginary part of the pair susceptibility acquires a universal form $\chi''(\omega, T) = T^\delta \mathcal{F}(\omega/T)$, with \mathcal{F} a generic scaling function, the exact form of which depends on the choice of different models. Here we choose in cases C-D-E $\delta = 1/2$, by construction. The weak coupling Fermi liquid BCS case A also shows scaling collapse at high temperatures, but with a marginal exponent $\Delta = 0$. In the quantum critical glue model (case B) energy-temperature scaling fails: for any choice of δ , at most a small fraction of the contour lines can be made vertical at high temperatures (here $\delta = 0$ is displayed).

new descriptions of the origin of superconductivity. The two cases D and E are the holographic analogues of local pair and “BCS” superconductors, in the sense that for the “large charge” case D the superconductivity sets in at a temperature of order of the chemical potential μ , while in the “small charge” case E the superconducting T_c is tuned to a temperature that is small compared to μ .

The remainder of this paper is organized as follows. In section II, we propose two explicit experimental approaches to measure the imaginary part of the pairing susceptibility in the required temperature and frequency range. One approach invokes modern thin film techniques and the other uses STM/STS/PCS techniques with a superconducting tip. Two heavy fermion systems, CeIrIn₅ and β -YbAlB₄, are suggested as candidate quantum critical superconductors. In section III, we present details of the calculation of the pairing susceptibility in the five types of models (A-E). For cases A-C, the full pair susceptibility is governed by the Bethe-Salpeter equation, with the bare (electronic) pair susceptibility and the pairing interaction (glue) as input. In the holographic approaches D and E, the pair susceptibility is calculated from the dynamics of the fluctuations of the dual scalar field in the AdS black hole background in the dual gravity theory. The outcomes of these calculations are further analyzed in section IV. Close to the superconducting transition point, all the five models display universal relaxational behavior. When moving away from T_c , one detects sharp qualitative differences between the truly conformal models (cases C-E) and the Hertz-Millis type models (case B). We include in Section V our conclusions. There are two appendix sections. In appendix A, the relaxational

behavior of the holographic models is derived using the near-far matching technique. In appendix B, we present a Hertz-Millis type calculation of the pair susceptibility in a marginal Fermi liquid.

II. PROPOSED EXPERIMENTAL SETUP

In order to experimentally observe $\chi_{\text{pair}}(\omega)$ via a second-order Josephson effect, one should measure the pair tunneling current, $I_{\text{pair}}(V) \propto \chi''_{\text{pair}}(\omega = 2eV/\hbar)$. This can be accomplished via a planar tunnel junction or weak link between the higher temperature superconductor (T_c^{high}) and the probe superconductor (T_c^{low}). To extract the pair tunneling current from the total tunneling current the quasiparticle tunneling current contribution must be subtracted, e.g., by means of the Blonder-Tinkham-Klapwijk³⁷ formula and its (*d*-wave) generalizations. To minimize the masking effect of the quasiparticle current and to maximize the ranges of accessible reduced temperature and frequency the ratio $T_c^{\text{high}}/T_c^{\text{low}}$ of the two T_c 's should be as large as possible.

Perhaps the best candidate quantum critical superconductor is the heavy fermion system CeIrIn₅, since it appears to have a quantum critical normal state at ambient pressure, while its T_c is a meager 0.4 K.³⁸ The mixed valence compound β -YbAlB₄, which displays quantum criticality up to about 3 K without any tuning and becomes superconducting below 80 mK,³⁹ is another possible choice. The challenge is now to find a good insulating barrier that in turn is well connected to a “high” T_c source superconductor. One option for the latter is the $T_c = 40$ K MgB₂ system; an added difficulty is that one should take care that this *s*-wave superconductor can form a Josephson contact with the non-conventional (presumably *d*-wave) quantum critical superconductor. This has on the other hand the great advantage that the quasiparticle current is largely suppressed because of the presence of the full gap, compared to an unconventional source superconductor with its nodal quasiparticles. As a start, one could employ the modern material fabrication techniques of monolithic molecular beam epitaxy (MBE)⁴⁰ and pulsed laser deposition (PLD),¹⁷ to form a junction between MgB₂ and Al with an insulating aluminum-oxide junction layer. Reduced temperatures $\tau = (T - T_c)/T_c$ up to 40 with low noise ω -values into the mV regime could be obtained with these two *s*-wave superconductors.

A more challenging technique is to utilize the recent advances in scanning tunneling microscopy and spectroscopy (STM/STS)⁴¹ and point contact spectroscopy (PCS)⁴² to form or glue a tiny crystal or whisker of YBa₂Cu₃O_{7-y} ($T_c^{\text{high}} = 90$ K) to a normal Ir or Pt tip and tunnel or weakly contact the tip to the heavy fermion superconductor through its freshly cleaved surface. With the enormous spread in transition temperatures τ -values of over 100 could be reached within a mV low-noise region for two such *d*-wave superconductors.

There are certainly difficulties with the cuprate superconductors such as surface charging, gap-reduction and low Josephson currents. These troublesome issues could be resolved by using a pnictide superconductor tip⁴³ or a combination of a hole-doped HTS (T_c^{high}) and concentration-tuned Nd_{2-x}Ce_xCuO_{4-δ} ($T_c^{\text{low}} < 24$ K), an electron-doped superconductor, to increase the Josephson current. Stimulated by our pair-susceptibility calculations, we trust the challenged experimentalists will evaluate the above possibilities in their efforts towards novel thin film and tunneling spectroscopy investigations.

III. CALCULATING THE PAIR SUSCEPTIBILITY FOR DIFFERENT MODELS

Cases A-C: Pairing mechanisms with electron-glue dualism

The pair susceptibility is a true two-particle quantity, i.e., it is derived from the full two-particle (four point) Green's function which is traced over external fermion legs: let $\chi(k, k'; q)$ be the full four-point correlation function with incoming momenta/frequencies $(-k, k+q)$ and outgoing momenta/frequencies $(-k', k'+q)$, then the pair susceptibility $\chi_{\text{pair}}(i\Omega, \mathbf{q}) = \sum_{k, k'} \chi(k, k'; q)$. Here momentum and frequency are grouped in a single symbol $k = (\mathbf{k}, i\omega)$ and we formulate equations using Matsubara frequencies.

The full pair susceptibility includes contributions from all forms of interactions. One commonly used approximation strategy is to separate it into two parts: an electronic part and a glue part. The glue is generally considered to be retarded in the sense that it has a characteristic energy scale ω_b that is small compared to the ultraviolet cut-off scale ω_c . Under this retardation assumption, i.e., a small Migdal parameter, the electron-glue vertex corrections can thus be ignored and the effects of the glue can be described by a Bethe-Salpeter-like equation in terms of the ‘vertex’ operators $\Gamma(k; q) = \sum_{k'} \chi(k, k'; q)$, i.e., a partial trace over $\chi(k, k'; q)$. Further simplification can be made by assuming that the pairing problem in quantum critical metals can still be treated within the Eliashberg-type theory, with the electronic vertex operator Γ_0 and the glue propagator D strongly frequency dependent, but without substantial momentum dependence. The glue part will only appear in the form of a frequency-dependent pairing

interaction $\lambda(i\Omega) = \int d^d \mathbf{q} D(\mathbf{q}; i\Omega)$. The Bethe-Salpeter equation (or Dyson equation for the four point function) then reads

$$\Gamma(i\nu; i\Omega) = \Gamma_0(i\nu; i\Omega) + \mathcal{A} \Gamma_0(i\nu; i\Omega) \sum_{\nu'} \lambda(i\nu' - i\nu) \Gamma(i\nu'; i\Omega), \quad (3)$$

at $\mathbf{q} = 0$. Note that the pair susceptibility is a bosonic response, hence $i\Omega$ is a bosonic Matsubara frequency whereas $i\nu$ is fermionic. For given electronic part $\Gamma_0(i\nu; i\Omega)$ and glue part $\lambda(i\Omega)$ equation (3) can be solved, either by iteration or by direct matrix inversion. A further frequency summation over ν of Γ finally yields the full pair susceptibility $\chi_{\text{pair}}(i\Omega, \mathbf{q} = 0) = \sum_{\nu} \Gamma(i\nu; i\Omega)$ at imaginary frequency $i\Omega$. The superconducting transition happens when the real part of the full pair susceptibility at $\Omega = 0$ diverges. To obtain the desired real-frequency dynamical pair susceptibility, a crucial step is the analytic continuation, i.e., the replacement $i\Omega \rightarrow \omega + i0^+$. We choose the method of analytic continuation through Padé approximants via matrix inversion,^{44–46} which performs remarkably well in our case, likely due to the fact that here the pair susceptibility is a very smooth function with only a single characteristic peak/feature.

Different models are characterized by different $\Gamma_0(i\nu; i\Omega)$ and $\lambda(i\Omega)$. We will present the three non-holographic approaches to pairing, i.e., cases A–C, in the remainder of this section.

1. Case A: Fermi liquid BCS

We consider a free Fermi gas, interacting via a normal glue, say an Einstein phonon, for which the pairing interaction is of the form

$$\lambda(i\Omega) = \frac{g}{\mathcal{A}} \frac{\omega_b^2}{\omega_b^2 + \Omega^2}. \quad (4)$$

For the Fermi gas Wick's theorem applies, and the electronic part of the pair susceptibility is simply the convolution of single-particle Green's functions,

$$\chi_{\text{pair},0}(\mathbf{q}, i\Omega) = \frac{T}{N} \sum_{\mathbf{k}, n} G(-\mathbf{k}, -i\nu_n) G(\mathbf{k} + \mathbf{q}, i\nu_n + i\Omega). \quad (5)$$

If we ignore self-energy corrections we may substitute the free fermion Green's function $G(\mathbf{k}, i\omega) = 1/(i\omega_n - \varepsilon_{\mathbf{k}})$. The imaginary part of the bare pair susceptibility then has the simple form $\chi_0''(\omega) = \frac{1}{\omega_c} \tanh\left(\frac{\omega}{4T}\right)$ at $\mathbf{q} = 0$. Here the Fermi energy acts as the ultraviolet cut-off, with $\omega_c = \frac{2}{\pi N(0)} \simeq E_F$. The electronic vertex operator reads

$$\Gamma_0(i\nu_n, i\Omega) = \frac{2T}{\omega_c(2\nu_n + \Omega)} [\theta(\nu_n + \Omega) - \theta(-\nu_n)] = \frac{2T}{\omega_c} \left| \frac{\theta(\nu_n + \Omega) - \theta(-\nu_n)}{2\nu_n + \Omega} \right|, \quad (6)$$

with $\theta(x)$ the Heaviside step function.

A full Eliashberg treatment includes self-energy corrections and modifies equation (6) to

$$\Gamma_0(i\nu_n, i\Omega) = \frac{2T}{\omega_c} \left| \frac{\theta(\nu_n + \Omega) - \theta(-\nu_n)}{(\nu_n + \Omega)Z(\nu_n + \Omega) + \nu_n Z(-\nu_n)} \right|, \quad (7)$$

where $\omega_n Z(\omega_n) \equiv \omega_n + \Sigma(i\omega_n)$. For small and non-singular pairing interaction $\lambda(i\Omega)$ the effect of the self-energy corrections will be minor.

2. Case B: Critical Glue BCS

In this subsection, we replicate one class of scenarios which attribute the novelty of unconventional superconductivity in such systems to the peculiar behavior of the glue when approaching the QCP. The glue part is assumed to become critical near the QCP, while the electronic part is kept a fermion bubble as in conventional BCS theory, equation (5), with self-energy corrections included. This class of scenarios are arguably best represented by the models introduced by Chubukov and collaborators,⁹ where they assume that pairing is mediated by a gapless boson, and the pairing interaction is of the power-law form

$$\lambda(i\Omega) = \left(\frac{\Omega_0}{|\Omega|} \right)^\gamma. \quad (8)$$

Here the exponent $0 < \gamma < 1$ parameterizes the different models. The pairing interaction has a singular frequency dependence, which makes the pairing problem in such models qualitatively different from that of the Fermi liquid BCS model. The coupling strength is absorbed in the parameter Ω_0 , which is the only scale-full parameter in this model. Thus the superconducting transition temperature should be proportional to Ω_0 , with a model-dependent coefficient, $T_c = A(\gamma)\Omega_0$.

The massless boson contributes a self-energy $\Sigma(i\omega_n)$ to the electron propagator,

$$\Sigma(i\omega_n) = \omega_n \left(\frac{\Omega_0}{|\Omega|} \right)^\gamma S(\gamma, n), \quad (9)$$

where $S(\gamma, n) = |n + 1/2|^{\gamma-1} [\zeta(\gamma) - \zeta(\gamma, |n + \frac{1}{2}| + \frac{1}{2})]$, with $\zeta(\gamma)$ the Riemann zeta function and $\zeta(\gamma, n)$ the generalized Riemann zeta function.

The presence of the scale-full parameter Ω_0 will generically prevent simple energy-temperature scaling of $\chi_{\text{pair}}(\omega, T)$. Only for the limits $T \ll \Omega_0$ or $T \gg \Omega_0$ one should recover energy-temperature scaling.

3. Case C: Quantum Critical BCS

In this subsection we will consider the scenario of quantum critical BCS,¹⁰ where the novelty of unconventional superconductivity is attributed solely to the peculiar behavior of the electronic part in the quantum critical region, with the glue part assumed featureless. For the glue part we will use, as in the Fermi liquid BCS case, the smooth and nonsingular pairing ‘Einstein phonon’ interaction, equation (4), to calculate the dynamical pair susceptibility in the QCBCS scenario. The quantum criticality is entirely attributed to the electronic part, i.e., the ‘bare’ pair susceptibility is assumed to be a conformally invariant state and is considered to be a relevant operator in the renormalization flow sense. In other words, this amounts to the zero temperature power-law form $\chi''_{\text{pair},0}(\omega, T=0) = \mathcal{A}\omega^{-\delta}$, with $0 < \delta < 1$. At finite temperature, the electronic part of the pair susceptibility can be expressed as a scaling function,

$$\chi_{\text{pair},0}(\omega, T) = \frac{Z}{T^\delta} \mathcal{F}\left(\frac{\omega}{T}\right), \quad (10)$$

which, in the hydrodynamical regime ($\hbar\omega \ll k_B T$) reduces to $\chi_{\text{pair},0}(\omega, T) = \frac{Z'}{T^\delta} \frac{1}{1 - i\omega\tau_{\text{rel}}}$, with $\tau_{\text{rel}} \approx \hbar/k_B T$. Note that the Fermi liquid is the corresponding marginal case $\delta = 0$ with $\chi''_{\text{pair},0}(\omega, T=0) \simeq \text{constant}$. With a relevant scaling exponent δ on the other hand, more spectral weight is accumulated at lower energy scales, where pairing is more effective. The gap equation becomes algebraic instead of exponential, and this implies that even a weak glue can give rise to a high transition temperature.

The QCBCS scenario is a phenomenological theory; in the absence of a microscopic derivation of the scaling function $\mathcal{F}(\omega/T)$ a typical functional form is chosen. One example of such a typical scaling function $\mathcal{F}(\omega/T)$ that possesses the above two limiting forms at low and high temperatures can be found in 1+1-dimensional conformal field theories, $\mathcal{F}''(y) = \sinh(\frac{y}{2})B^2(s + i\frac{y}{4\pi}, s - i\frac{y}{4\pi})$, where B is the Euler beta function, and $s = 1/2 - \delta/4$. Another example, which will be used to calculate the full pair susceptibility in this paper, is a simple generalization of the free fermion vertex operator, equation (6),

$$\Gamma_0(i\nu_n, i\Omega) = \frac{(1-\alpha)T}{\omega_c^{1-\alpha}} \frac{|\theta(\nu_n + \Omega) - \theta(-\nu_n)|}{|2\nu_n + \Omega|^{\alpha+1}}, \quad (11)$$

$$\chi_{\text{pair},0}(i\Omega) = \sum_{\nu_n} \Gamma_0(i\nu_n, i\Omega) = \frac{(1-\alpha)T}{\omega_c^{1-\alpha}} \frac{2}{(4\pi T)^{1+\alpha}} \zeta\left(1+\alpha, \frac{1}{2} - i\frac{i\Omega}{4\pi T}\right). \quad (12)$$

Here ζ is again the generalized (Hurwitz) zeta function. Since analytic continuation is trivial it is easy to confirm that this choice of vertex operator produces a relevant bare pair susceptibility with $\delta = \alpha$, a power-law tail at high frequency, and the linear hydrodynamic behavior at low frequency. There is a single peak at frequencies of order the temperature, the precise location of which we may fine-tune by introducing a parameter x_0 (defined as the argument of the scaling function $\mathcal{F}(x)$ at which the low-frequency linear and high frequency power-law asymptotes would cross).

We would like to emphasize again that QCBCS is a phenomenological theory: equation (11) is an educated guess for what a true conformally invariant two-particle correlation function (partially traced) may look like. However, combined with a glue function, equation (4), it is perfectly valid input for the Eliashberg framework, i.e., the Bethe-Salpeter equation (3), and delivers quite a high T_c .

Cases D-E: Holographic superconductivity

In the holographic approach to superconductivity the 2+1 dimensional conformal field theory (CFT) describing the physics at the quantum critical point is encoded in a 3+1 dimensional string theory in a spacetime with a negative cosmological constant (anti-de Sitter space).^{33–35} In a “large N , strong coupling limit” this string theory can be approximated by classical general relativity in an asymptotically anti-de Sitter (AdS) background coupled to various other fields. Most importantly, a precise dictionary exists how to translate properties of the AdS gravity theory to properties of the CFT including the partition function. In particular, a global symmetry in the CFT is a local symmetry in the gravity theory with the boundary-value of the gauge field identified with the source for the current in the CFT. This provides the set-up for holographic superconductivity in the standard approximation where superconductivity is studied as the spontaneous symmetry breaking of a global $U(1)$, that is subsequently weakly gauged to dynamical electromagnetism.

4. Case D: “Large charge” AdS_4 holographic superconductor

The simplest model to obtain a holographic superconductor is therefore Einstein gravity minimally coupled to a $U(1)$ Maxwell field A_μ and a charged complex scalar Ψ with charge e and mass m .^{11,36,47} The charged scalar will be dual to the order parameter in the CFT — the pairing operator. Since the underlying field theory is strongly coupled there is no sense in trying to identify the order parameter as some “weakly bound” pair of fermions and we ought to study the order parameter directly.

This system has the action

$$S_0 = \int d^4x \sqrt{-g} \left[R + \frac{6}{L^2} - \frac{1}{4} F_{\mu\nu} F^{\mu\nu} - m^2 |\Psi|^2 - |\nabla^\mu \Psi - ie A^\mu \Psi|^2 \right], \quad (13)$$

where R is the Ricci scalar and the AdS radius L can be set to 1. The charged AdS Reissner-Nordström (RN) black hole is a solution with $\Psi = 0$. This solution has the spacetime metric and electrostatic potential

$$\begin{aligned} ds^2 &= -f(r) dt^2 + \frac{dr^2}{f(r)} + r^2(dx^2 + dy^2), \\ f(r) &= r^2 - \frac{1}{r} \left(r_+^3 + \frac{\rho^2}{4r_+} \right) + \frac{\rho^2}{4r^2}, \\ A &= \rho \left(\frac{1}{r_+} - \frac{1}{r} \right) dt, \end{aligned} \quad (14)$$

where r_+ is the position of the horizon and ρ corresponds to the charge density of the dual field theory. The temperature of the dual field theory is identified as the Hawking temperature of the black hole $T = \frac{3r_+}{4\pi} \left(1 - \frac{\rho^2}{12r_+^4} \right)$, and the chemical potential is $\mu = \rho/r_+$. The AdS-RN solution preserves the $U(1)$ gauge symmetry and corresponds holographically to the CFT in a state at finite temperature and chemical potential.

The essence of holographic superconductivity is that below some critical temperature T_c , the charged AdS-RN black hole becomes unstable and develops a non-trivial (normalizable) scalar condensate, i.e., $\Psi \neq 0$, which breaks the $U(1)$ gauge symmetry. The asymptotic $r \rightarrow \infty$ value of Ψ is the value of the order parameter in the CFT. Thus in the dual field theory a global $U(1)$ symmetry is broken correspondingly. Such a minimal model therefore naturally realizes (*s-wave*) superconductivity.^{11,36}

Using explicit details of the AdS/CFT dictionary, the dynamical susceptibility of the spin-zero charge-two order parameter \mathcal{O} in the boundary field theory can be calculated from the dynamics of the fluctuations of the corresponding scalar field Ψ in the AdS black hole background in the gravity side. At zero momentum, we can expand $\delta\Psi$ as $\delta\Psi(r, x, y, t)|_{k=0} = \psi(r) e^{-i\omega t}$. The equation of motion for $\psi(r)$ is

$$\psi'' + \left(\frac{f'}{f} + \frac{2}{r} \right) \psi' + \left(\frac{(\omega + eA_t)^2}{f^2} - \frac{m^2}{f} \right) \psi = 0. \quad (15)$$

We are interested in the retarded Green’s function. This translates into imposing infalling boundary condition at the horizon,⁴⁸ i.e., $\psi(r) \simeq (r - r_+)^{-i\frac{\omega}{4\pi T}}$, as $r \rightarrow r_+$. The CFT Green’s function is then read off from the behavior of solutions ψ_{sol} to (15) at spatial infinity $r \rightarrow \infty$. Near this AdS boundary, one has $\psi(r) \simeq \frac{\psi_-}{r^{\Delta_-}} + \frac{\psi_+}{r^{\Delta_+}}$, where $\Delta_\pm = \frac{3}{2} \pm \nu$ with $\nu = \frac{1}{2}\sqrt{9 + 4m^2}$. We focus on the case $0 < \nu < 1$, where both modes ψ_\pm are normalizable. We furthermore

choose “alternate quantization” with ψ_+ as the source and ψ_- as the response, such that in the large frequency limit the order parameter susceptibility behaves as $1/\omega^{2\nu}$. In that case, the Green’s function is given by^{48,49}

$$\chi_{\text{pair}} = \mathcal{G}_{\mathcal{O}_-^\dagger \mathcal{O}_-}^R \sim -\frac{\psi_-}{\psi_+}. \quad (16)$$

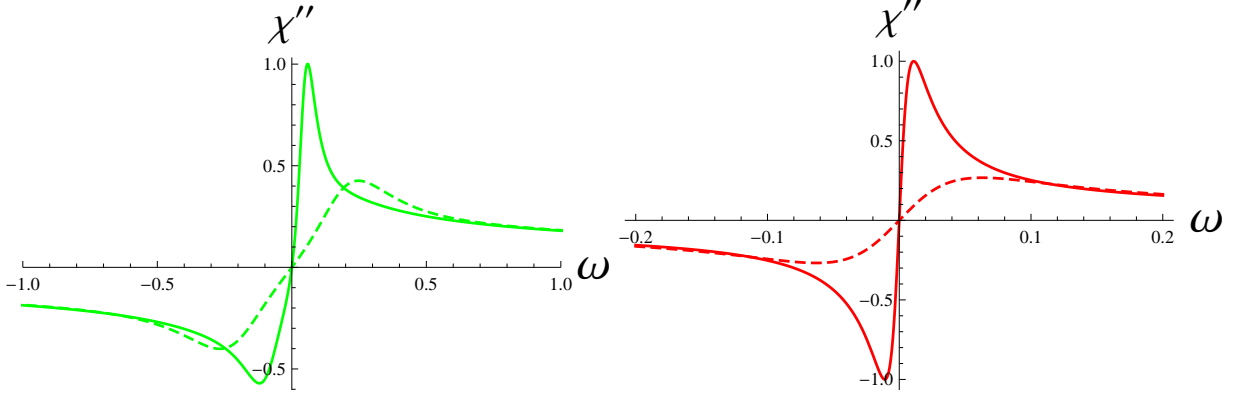


FIG. 3: (Color online) **Particle-hole (a)symmetry of the relaxational peak.** Particle-hole (a)symmetry as seen from the line shape of $\chi''(\omega)$ for the two different kinds of holographic superconductors: local pair AdS_4 (left) and BCS-type AdS_2 (right). The solid lines correspond to reduced temperature $\tau = (T - T_c)/T_c = 1$ and the dashed lines correspond to $\tau = 5$. The AdS_4 case has a particle-hole asymmetric pair susceptibility, while this symmetry is restored in the AdS_2 case.

From equation (15), the boundary conditions at the horizon and the dictionary entry for the Green’s function, the order parameter susceptibility has the manifest symmetry $\chi(\omega, e) = \chi^*(-\omega, -e)$. This implies generic particle-hole asymmetry as for $e \neq 0$ $\chi(\omega, e)$ is generally asymmetric under the transformation $\omega \rightarrow -\omega$, as has been predicted for phase fluctuating superconductors.¹⁸ Only in the zero charge limit is particle-hole symmetry restored (Fig. 3).

5. Case E: “Small charge” AdS_2 holographic superconductor

The AdS -RN black hole at $T = 0$ has a near-horizon $r \rightarrow r_+ = (12)^{-1/4} \sqrt{\rho}$ limit that corresponds to the geometry of $\text{AdS}_2 \times R^2$. This radial distance in AdS characterizes the energy-scale at which the CFT is probed, and one can show that fermionic spectral functions that have the same phenomenology as the strange metallic behavior observed in condensed matter systems arise from gravitational physics in this near horizon AdS_2 region.⁵⁰ It is therefore of interest at which temperature the superconducting instability sets in.

In the case D simplest “large-charge” holographic superconductor all dimensionfull constants are of order one. Thus $T_c \sim \mu$ and the onset of superconductivity happens before one is essentially probing the near-horizon physics.⁵⁷ To access the AdS_2 near-horizon geometry we wish to tune T_c as low as possible. This can be realized by combining a double trace deformation in the CFT with a non-minimal “dilaton-type” coupling in the gravity theory.¹² When the order parameter \mathcal{O} has scaling dimension $\Delta_- < 3/2$, $\mathcal{O}^\dagger \mathcal{O}$ is a relevant operator, and the IR of the field theory can be driven to a quantitatively different T_c /qualitatively different state by adding this relevant operator as a deformation

$$S_{\text{FT}} \rightarrow S_{\text{FT}} - \int d^3x \tilde{\kappa} \mathcal{O}^\dagger \mathcal{O}, \quad (17)$$

where $\tilde{\kappa} = 2(3 - 2\Delta_-)\kappa$. See Fig. 4. This operation does not change the bulk action, but now we need to study the bulk gravitational theory using new boundary conditions for the scalar field. The retarded Green’s function becomes⁵¹

$$G_R \sim \frac{\psi_-}{\kappa\psi_- - \psi_+}, \quad (18)$$

and the susceptibility can be shown to take the Dyson-series RPA form:

$$\chi_\kappa = \frac{\chi_0}{1 + \kappa\chi_0}. \quad (19)$$

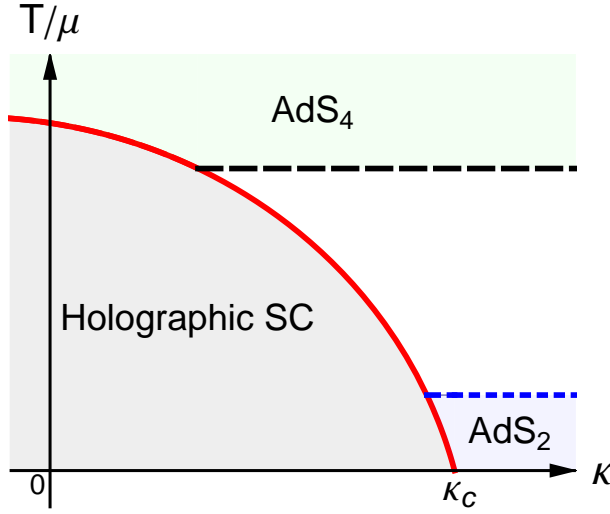


FIG. 4: (Color online) **A phase diagram of holographic superconductor including a double-trace deformation with strength κ .** For $\kappa = 0$ one has the minimal holographic superconductor, case D, where $T_c \sim \mu$. Increasing the value of κ can decrease the critical temperature all the way to $T_c = 0$ if one includes a non-minimal coupling to the AdS-gauge field (see text). The shaded regions indicate which region of the geometry primarily determines the susceptibility. It shows that one must turn on a double-trace coupling to describe superconductors whose susceptibility is determined by AdS₂-type physics. This is of interest as AdS₂-type physics contains fermion spectral functions that are close to what is found experimentally.

This already modifies T_c but it can be further reduced by adding an extra “dilaton-type” coupling $|\Psi|^2 F^2$ term to the minimal model action in equation (13),¹²

$$\mathcal{S}_1 = -\frac{\eta}{4} \int d^4x \sqrt{-g} |\Psi|^2 F_{\mu\nu} F^{\mu\nu}. \quad (20)$$

In the normal phase, the AdS RN black hole, equation (14), is still a solution to this action. The susceptibility again follows from the Green’s function (18) in this background, which is built from solutions to the equation of motion for $\delta\Psi(r, x, y, t)|_{k=0} = \psi(r)e^{-i\omega t}$. With the two modifications (17) and (20) it equals

$$\psi'' + \left(\frac{f'}{f} + \frac{2}{r}\right)\psi' + \left(\frac{(\omega + eA_t)^2}{f^2} + \frac{\eta\rho^2}{2r^4 f} - \frac{m^2}{f}\right)\psi = 0. \quad (21)$$

IV. RESULTS AND DISCUSSIONS

Let us now explain why the experiment needs to cover a large range of temperatures and frequencies in order to extract the differences in physics. The thermal transition to the superconducting state is in all cases a “BCS-like” mean field transition — for A–C this is by construction, involving large coherence lengths, but for the holographic superconductors it is an outcome that is expected but not completely understood. As in all critical phenomena, the mean-field universal behavior sufficiently close to the phase transition to the superconducting state is given by standard Ginzburg-Landau order parameter theory,

$$\mathcal{L} = \frac{1}{\tau_r} \Psi \partial_t \Psi + |\nabla \Psi|^2 + i \frac{1}{\tau_\mu} \Psi \partial_t \Psi + \alpha_0 (T - T_c) |\Psi|^2 + w |\Psi|^4 + \dots \quad (22)$$

Evaluating the order parameter susceptibility in the normal state one finds,

$$\chi_{\text{pair}}(\omega, T) = \frac{\chi'_{\text{pair}}(\omega = 0, T)}{1 - i\omega\tau_r - \omega\tau_\mu}, \quad (23)$$

Indeed in all cases Fig. 5a shows the familiar “Curie-Weiss” behavior $\chi'_{\text{pair}}(\omega = 0, T) = 1/[\alpha_0(T - T_c)]$, at temperatures $T_c \leq T \lesssim 3T_c$, with relaxation time $\tau_r \propto (T - T_c)^{-1}$. The time τ_μ measures the breaking of the charge conjugation symmetry at the transition. In the relaxational regime, the tunneling current signal obtains the quasi-Lorentzian

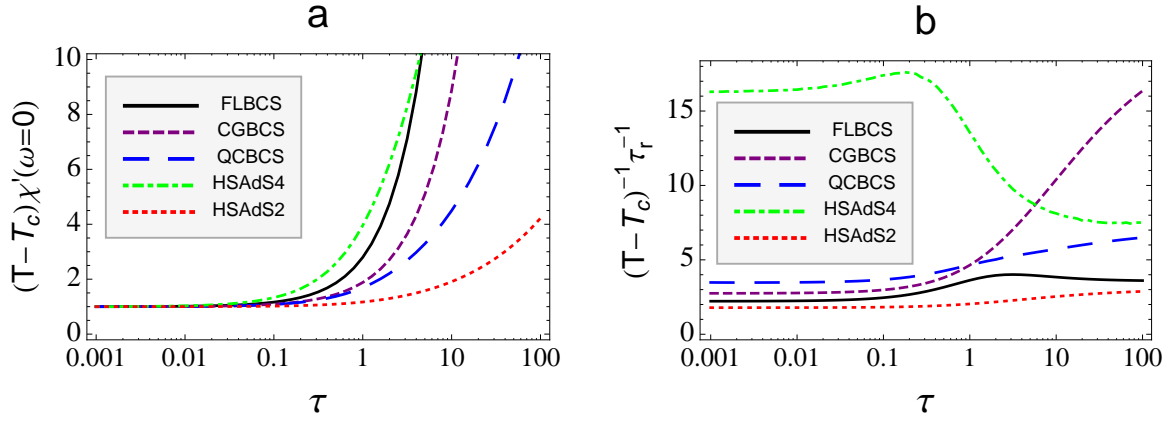


FIG. 5: (Color online) **The universal mean field behavior of the pair susceptibility close to the superconducting phase transition.** **a**, Plot of the real part of the pair susceptibility at zero frequency rescaled by the distance to the superconducting transition point, i.e., $(T - T_c)\chi'(\omega = 0, T)$, as function of reduced temperature $\tau = (T - T_c)/T_c$, for the five different models considered. The horizontal axis is plotted on the logarithmic scale, and we use the normalization $(T - T_c)\chi'(\omega = 0, T) \rightarrow 1$ as $T \rightarrow T_c$. $\chi'(\omega = 0)$ is a measure of the overall magnitude of the pair susceptibility in arbitrary units. $\chi'(\omega = 0, \tau)$ can be determined from the experimentally measured imaginary part of the pair susceptibility by using the Kramers-Kronig relation $\chi'(\omega = 0, T) = \frac{1}{\pi} \int d\omega \chi''(\omega, T)/\omega$. **b**, the inverse relaxation time τ_r rescaled by the distance to the superconducting transition point, i.e., $(T - T_c)^{-1}\tau_r^{-1}$, as function of reduced temperature τ . The horizontal axis is also plotted on the logarithmic scale. The relaxation time is calculated from the relation $\tau_r = [\partial\chi''/\partial\omega]_{\omega=0}/\chi'(\omega = 0)$ (see text for equations). In both plots, for all the five different models A-E, the curves become flat close to the transition temperature T_c (here for $\tau \lesssim 0.1$), i.e., both $\chi'(\omega = 0, T)$ and $\tau_r(T)$ behave as $1/(T - T_c)$, confirming the universal mean field behavior in this regime. We also see from **b** that the “large charge” holographic superconductor (here with charge $e = 5$) has a much shorter relaxation time than the “small charge” holographic superconductor (here with charge $e = 0$).

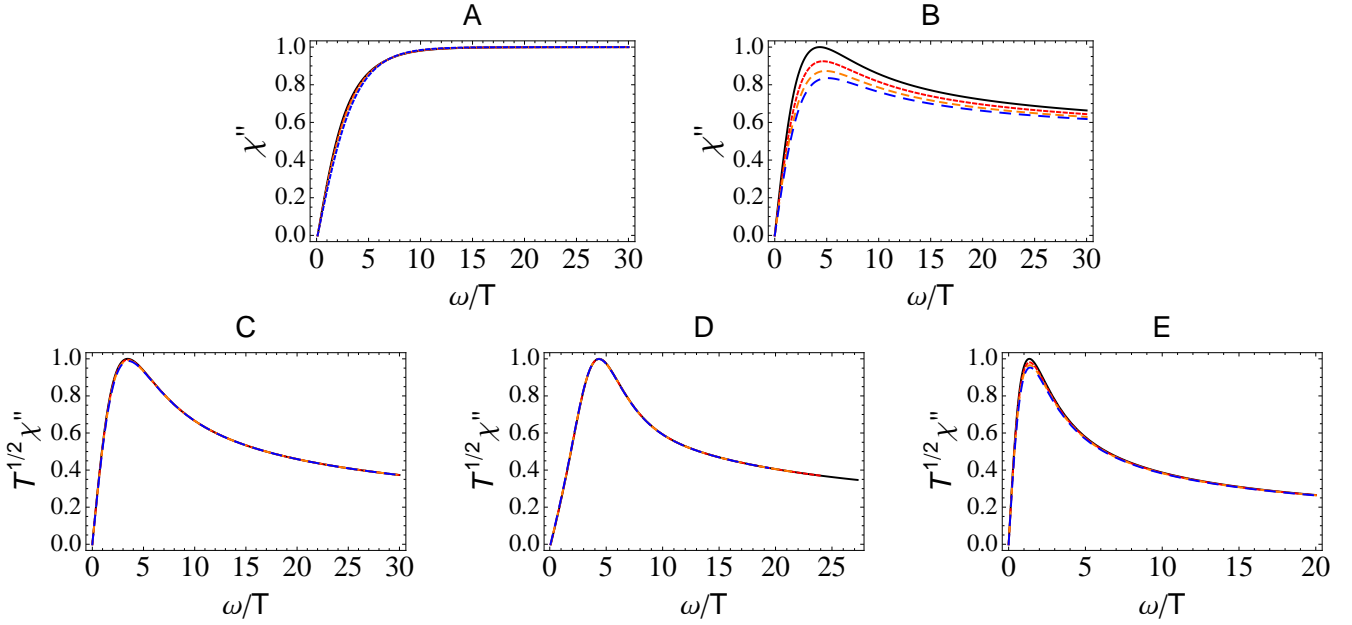


FIG. 6: (Color online) **Energy-temperature scaling line cuts.** **A-E**, High temperature line cuts of the imaginary part of the pair susceptibility rescaled by temperature to a certain power: $T^\delta\chi''$, as function of ω/T for the five different cases. Here in each figure we have plotted four different temperatures, with reduced temperatures $\tau = 21, 24, 27, 30$. As the vertical contour lines in Fig. 3 already revealed, the cases A, C, D and E exhibit a scaling collapse at high temperatures, whereas scaling collapse fails in the “Hertz-Millis-Chubukov” case B. Furthermore, the line shape is quite different in cases C, D and E as compared to cases A and B. For C, D and E, $\chi''(\omega, T)$ decays as power law at high temperatures whereas for A and B $\chi''(\omega, T)$ approaches the Fermi liquid tanh-form in the high temperature limit. The pronounced peak in cases C, D and E versus the flatness of A and B is signified by a plot of the full width at half maximum (see Fig. 7).

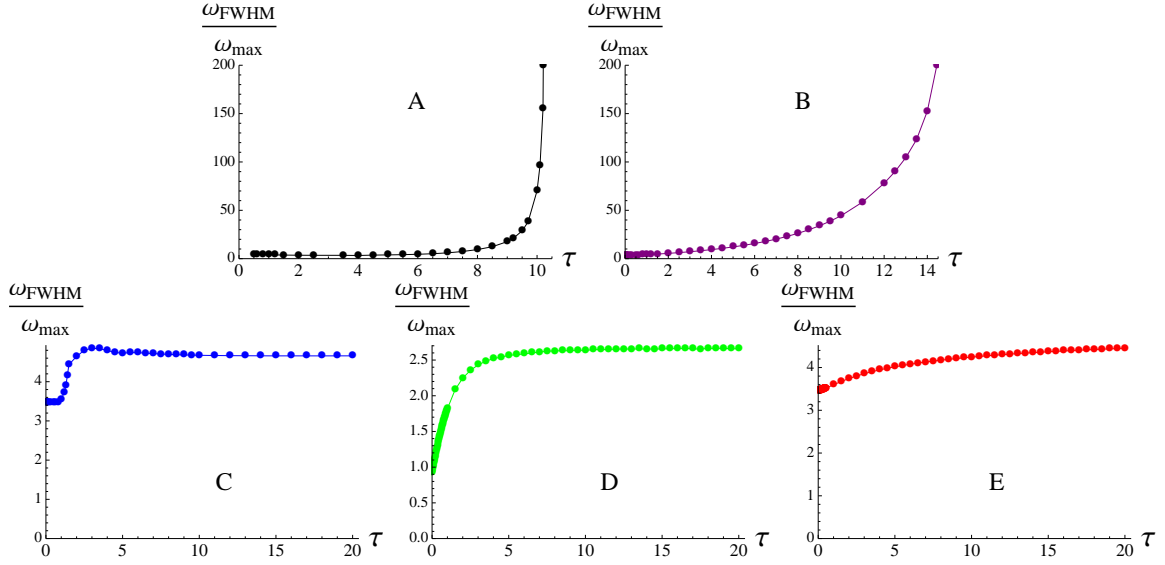


FIG. 7: (Color online) **Peak width crossover.** Evolution of the relative peak width, i.e., the ratio of the full width at half maximum (FWHM) of the peak and peak location ω_{\max} , as a function of reduced temperature $\tau = (T - T_c)/T_c$ for the five different models. For FLBCS (A) and CGBCS (B), the ratio diverges at high temperature. For QCBCS (C) there is a sudden change from the low temperature relaxational behavior to the high temperature conformal field theory behavior. For the two holographic superconductors (D–E), the crossover from high temperature region to low temperature region is more smooth.

lineshape $\chi''_{\text{pair}}(\omega) = \chi'(0)\tau_r\omega/[\tau_r^2\omega^2 + (1 - \tau_\mu\omega)^2]$. Since cases A–C are strongly retarded, charge conjugation is effectively restored (i.e., $\tau_\mu = 0$) for the usual reason that the density of fermionic states is effectively constant (or symmetric, case C) around E_F . As for phase-fluctuating local pairs, the ‘strongly coupled’ holographic superconductor D shows a quite charge-conjugation asymmetric result, $\tau_\mu/\tau_r \approx 0.4$, while it is remarkable that the “weakly coupled” holographic case E displays a near complete dynamical restoration of charge conjugation ($\tau_\mu/\tau_r \approx 0$) (see Fig. 3).

In the Landau-Ginzburg regime the order parameter relaxation time τ_r does still give us a window on the underlying fundamental physics. Strongly coupled quantum critical states are characterized by a fundamental “Planckian” relaxation time $\tau_h = A\hbar/(k_B T)$ and the order parameter fluctuations in the normal state ought to submit to this universal relaxation. For rather elegant reasons this is the case in the holographic superconductors (D,E) (see Appendix A). One finds that $\tau_r = A_{D/E}\hbar/[k_B(T - T_c)]$, where $A_D \approx 0.06$, $A_E \approx 1.1$ (“zero temperature” equals T_c for the order parameter susceptibility). Not surprisingly this works in a very similar way for case C but viewed from this quantum critical angle the textbook BCS result that $\tau_r = (\pi/8)\hbar/[k_B(T - T_c)]$ is rather astonishing. Although the underlying Fermi-liquid has a definite scale E_F (e.g., its relaxation time is $\tau_{\text{FL}} = (E_F/k_B T)\tau_h$) its pair channel is governed by effective conformal invariance, actually in tune with the quantum critical BCS moral.

Given this “quasi-universality” near the phase transition, one has to look elsewhere to discern the pairing mechanism from the information in the pair susceptibility. It is obvious where to look: Fig. 1 shows that the differences appear at temperatures large compared to T_c involving a large dynamical range in frequency. This is the challenge for the experimental realization. In this large dynamical range one distinguishes directly all quantum critical cases (B–E) for which the contour lines in Fig. 1 acquire a convex shape, from simple BCS with fanning-out contours. One sees the reasons for this more clearly in figures 2 and 6, which plot $T^\delta\chi''_p(\omega/T, \tau)$, i.e., a rescaling by temperature. Figure 2 displays the same temperature range as in figure 1, figure 6 shows several line-cuts at high temperatures. In the simple BCS case A the high temperature pair susceptibility is just the free Fermi gas result $\chi''(\omega, T) = (1/E_F)\tanh(\omega/4T)$, linearly increasing with frequency initially and becoming constant for $\omega > 8T$. In cases B–E the pair susceptibility deep in the normal state increases with decreasing frequency down to a scale set by temperature to eventually go to zero linearly at small frequency as required by hydrodynamics. The observation of such a behavior would reveal a significant clue regarding a non conventional origin of the superconductivity. The frequency independence of $\chi''_{\text{BCS}}(\omega)$ reveals the “marginal” scaling that is equivalent to the logarithmic singularity in $\chi'(\omega = 0)$ that governs the BCS instability. In contrast, the critical temperature peak in $\chi''(\omega)$ in cases B–E reveals a “relevant” scaling behavior in the pair channel: a stronger, algebraic singularity is at work giving away that the quantum critical electron system is intrinsically supporting a more robust superconductivity than the Fermi gas.

The observation of such a peak implies that one can abandon the search for some “super glue” that enforces pairing

in the Fermi gas at a “high” temperature. Instead the central question becomes: what is the origin of the relevant scaling flow in the pair channel in the normal state, and is the normal state truly quantum critical in the sense of being controlled by conformal invariance? Fig. 4 shows that, if it is, the pair susceptibility must display energy-temperature scaling in this high temperature regime. Both the quantum critical BCS (C) and the two holographic cases (D,E) embark from the assumption that the high temperature metal is governed by a strongly interacting quantum critical state that is subjected to the hyper-scaling underlying the energy-temperature scaling collapse. Specifically the pair operator itself is asserted to have well-defined scaling properties, as in 1+1-dimensional Luttinger liquid. Such “truly” quantum critical metals have no relation whatever with the Fermi liquid, but this is not quite the case for the Hertz style critical glue case (B). Although the fully re-summed Eliashberg treatment of the strongly coupled “singular glue” $\lambda(\omega) \sim 1/\omega^\gamma$ completely changes the pair susceptibility relative to the simple BCS case it is still a perturbative theory around the Fermi-liquid. It remembers that it is based on a Fermi liquid with a characteristic scale E_F and this prohibits the energy temperature scaling, as illustrated in Figs 2B, 6B.

The observation of energy-temperature scaling in the high temperature pair susceptibility would therefore reveal the existence of a true non-Fermi liquid quantum critical state formed from fermions. Although it remains to be seen whether it has any bearing on the condensed matter systems, the only controlled mathematical theory that is available right now to deal with such states of matter is the AdS/CFT correspondence of string theory. It has its limitations: the “bottom up” or “phenomenological” approach of relevance in the condensed matter context should be regarded as a generalized scaling theory, which reveals generic renormalization flows associated with strongly interacting quantum critical states encountered in the presence of fermions at a finite density. However, the scaling dimensions, rates of relevant flows and so forth associated with a particular theory/universality class are undetermined in this bottom up approach. Cases D and E are two limiting cases of such generic RG flows. The “large charge” case D departs from a “primordial” Lorentz invariant critical state at zero density (encoded in an AdS_4 geometry in the gravitational dual) that is natural in supersymmetric quantum field theory while it is far fetched as a UV theory for condensed matter systems. A better holographic contender for condensed matter physics is case E. Here the holographic superconductivity is governed by the emergent quantum criticality associated with the near horizon AdS_2 geometry of the extremal Reissner-Nordstrom black hole. This is dual to an (unstable) infrared fixed point where the normal state shows the traits of the marginal Fermi liquid.⁵²

For the pair susceptibilities the distinction between case D and E is only quantitative at zero momentum, associated with a choice of different scaling dimensions. The crucial difference is with the other scenarios. In the holographic cases no “external glue” is at work. The superconducting instability is an intrinsic property associated with the strongly coupled fermionic critical matter. As can be seen directly from the pair susceptibilities in Figs. 2D, 2E, the superconducting correlations builds up through a very smooth but rapid flow from the conformal high temperature regime to the relaxational regime associated with the thermal transition. The smoothness of the flow towards the instability is also emphasized when one considers more closely the way that the relaxational peak morphs into the conformal peak as function of temperature: in the QCBCS case this can be relatively sudden given that scale is introduced through the characteristic glue energy, while in both the AdS_4 and AdS_2 cases this is just a very smooth cross over flow (see Fig. 7).

V. CONCLUSIONS

In this paper we demonstrated, through explicit calculations of the pairing susceptibility in five different models, the existence of sharp qualitative difference between the truly quantum critical models — phenomenological QCBCS or the holographic models — and the Hertz-Millis type models with respect to energy-temperature scaling. In the Hertz-Millis type models for pairing, the pairing channel is assumed to be secondary. The single particle Green’s functions, and/or certain bosonic quantities in the particle-hole channel, e.g. magnetic susceptibilities, are considered to be primary and carry the criticality, enjoying energy-temperature scaling. The pairing susceptibility is assumed to be a derived quantity, and it remains sensitive to the underlying Fermi-energy. Thus generally one does not expect to have energy-temperature scaling in the pairing channel, or at the best scaling can only occur with extreme fine tuning. The essence of QCBCS and the holographic approach is to take the superconducting order parameter itself to be a conformal field in the quantum critical region. This is the underlying reason for energy-temperature scaling in these models. The observation of energy-temperature scaling with an obviously nonzero scaling exponent in the pairing susceptibility would unambiguously reveal the non-BCS nature of the pairing mechanism and the non-Hertz-Millis nature of the quantum critical state. The contrast between superconductivity emerging from a strongly interacting fermionic quantum critical state and any mechanism that sets out from a Fermi-liquid is qualitatively so different that the proposed experiment might finally settle the basic rules associated with superconductivity in quantum critical systems.

Acknowledgements

We would like to acknowledge Jan Aarts, Mihailo Čubrović, J. C. Seamus Davis, Dimitrios Galanakis, Sean A. Hartnoll, Hans Hilgenkamp, Mark Jarrell, Sergei I. Mukhin, Andrei Parnachev, Catherine Pepin, Jan van Ruitenbeek and Jian-Xin Zhu for stimulating discussions. This research was supported in part by a VIDI Innovative Research Incentive Grant (K. Schalm) from the Netherlands Organisation for Scientific Research (NWO), a Spinoza Award (J. Zaanen) from the Netherlands Organisation for Scientific Research (NWO) and the Dutch Foundation for Fundamental Research on Matter (FOM).

Appendix A: Relaxational behavior in holographic superconductors: near-far matching

A remarkable aspect of the AdS/CFT computation is that the relaxational behavior is directly encoded in the geometry. Near $\omega \rightarrow 0$ an analytic expression for the Green's function follows from a near-horizon/AdS-boundary matching method first used in ref. 50. The result is that for $\omega \rightarrow 0$, the Green's function is of the form

$$G_R(\omega, T, e) \sim \frac{b_+^{(0)} + b_+^{(1)}\omega + \mathcal{O}(\omega^2) + \mathcal{G}(\omega, T)(b_-^{(0)} + b_-^{(1)}\omega + \mathcal{O}(\omega^2))}{a_+^{(0)} + a_+^{(1)}\omega + \mathcal{O}(\omega^2) + \mathcal{G}(\omega, T)(a_-^{(0)} + a_-^{(1)}\omega + \mathcal{O}(\omega^2))}, \quad (\text{A1})$$

where $\mathcal{G}(\omega, T)$ is the near-horizon “IR-CFT” Green's function defined in a similar way as the full “AdS-CFT” Green's function, i.e., it is the ratio of leading and subleading coefficients at the boundary of the near-horizon region of a solution to the equation of motion. The coefficients $a_\pm^{(n)}(e, T)$, $b_\pm^{(n)}(e, T)$ are determined by matching this IR-solution to the “UV”-solution near the AdS-boundary at spatial infinity. They can only be obtained numerically. Note that when $e = 0$ particle-hole symmetry dictates that in that case $a_\pm^{(1)} = b_\pm^{(1)} = 0$.

As G_R is the Green's function for the order parameter it must develop a pole at $\omega = 0$ for $T = T_c$. Thus when $T \rightarrow T_c$, $\omega \rightarrow 0$, the Green's function, equation (A1), takes the form

$$G_R(\omega, T, e) \sim \frac{\gamma_0}{\beta_0(T - T_c) + i\omega\beta_1 + \omega\beta_2}, \quad (\text{A2})$$

where $\gamma_0 = b_+^{(0)}(e, T_c)$, $\beta_0 = \partial_T a_+^{(0)}(e, T_c)$, $\beta_1 = \lim_{\omega \rightarrow 0} \frac{1}{i\omega} \mathcal{G}(\omega, T_c) a_-^{(0)}(e, T_c)$ and $\beta_2 = a_+^{(1)}(e, T_c)$. Comparing to the universal relaxational behavior of the susceptibility (equation (6) in the main text)

$$\chi(\omega, T) = \frac{\chi'(\omega = 0, T)}{1 - i\omega\tau_r - \omega\tau_\mu} \quad (\text{A3})$$

we recognize the Curie-Weiss susceptibility $\chi'(\omega = 0, T) = \frac{\gamma_0}{\beta_0(T - T_c)}$, and the particle-hole asymmetry parameter $\tau_\mu = -\frac{\beta_2}{\beta_0(T - T_c)}$, which indeed vanishes when $e = 0$. But most interestingly the relaxation time

$$\tau_r = \lim_{\omega \rightarrow 0} \frac{i}{\omega\beta_0(T - T_c)} \mathcal{G}(\omega, T_c) a_-^{(0)}(e, T_c) \quad (\text{A4})$$

is directly given in terms of the IR Green's function $\mathcal{G}(\omega, T)$. The AdS gravity response function therefore directly knows about the relaxational dynamics in the dual conformal field theory.

There are essentially two different regimes of interest

1. For $\omega \ll T$, the near-horizon IR Green's function takes the universal form $\mathcal{G}(\omega, T) = -i\omega/4\pi T$. Thus $\tau_r = \alpha_0/(T - T_c)$. This is gravity version of the universal relaxation that for $\omega \ll T$, $\chi'' = \text{Im}G_R$ should always be linear in ω . (This frequency regime applies to both case D and E.)
2. For $T \ll \omega \ll \sqrt{\rho}$, the IR Green's function is completely determined by the $SO(1, 2)$ conformal symmetry of the near-horizon $T \simeq 0$ AdS₂ region. As a consequence the IR Green's function must be a power law in frequency:

$$\mathcal{G} \sim \omega^{\delta_+ - \delta_-}, \quad (\text{A5})$$

where δ_\pm are the two possible IR-conformal dimensions of the scalar field controlled by its dynamics the AdS₂ geometry, and we focus on real δ_\pm .⁵⁰ In terms of the parameters explained in the Case E subsection (see equation (21)) these conformal dimensions are

$$\delta_\pm = \frac{1}{2} \pm \sqrt{\frac{1}{4} + 2r_+^4 m^2 - 4r_+^4 e^2 - \eta}, \quad (\text{A6})$$

For this range of frequencies the susceptibility will therefore also exhibit scaling but with non-“Curie-Weiss” exponents: $\chi'' \sim \omega^{-\delta_+ + \delta_-}$. (This frequency regime only applies to case E. For case D the temperature $T_c \simeq \mu \sim \sqrt{\rho}$ and T cannot be much smaller than $\sqrt{\rho}$ in the normal state.)

For $\omega \gg \sqrt{\rho}$, one is outside of the regime of validity of (A2). Indeed there is no “relaxation” for such high frequencies. Instead the Green’s function is now determined by the UV-theory and all temperature/chemical potential effects are subleading. In this case the UV-theory is a 2+1 dimensional CFT dual to AdS_4 and the two-point correlation function is completely fixed by the $SO(3,2)$ symmetry $\chi'' \sim 1/\omega^{2\nu}$ where $\nu = \frac{1}{2}\sqrt{9 + 4m^2}$. (Recall from equation (15) that we are using “alternate quantization”. For “standard quantization” one would have $\chi'' \sim \omega^{2\nu}$.)

Appendix B: Pairing with Marginal Fermi liquid

To illustrate how powerful and universally distinctive the qualitative differences in energy-temperature scaling are, we study here the pair susceptibility of the Marginal Fermi liquid (MFL) which has been a prime candidate for some strange metallic states. A further motivation is that recent numerical calculations^{28,29} found quantum critical scaling for a MFL when combined with a van Hove singularity (vHS).

We first calculate the pairing susceptibility built out of a fermion bubble with MFL self-energy and a smooth density of states (DOS). Both a smooth BCS type pairing glue and a quantum critical glue are considered. We find that for both types of pairing interactions, energy-temperature scaling is severely broken, exhibiting clear distinction with QCBSC and the holographic approach. When now combined with an extended van Hove singularity, MFL can produce a “quasi-conformal” pair susceptibility,^{28,29} but extreme fine tuning is required. The vHS has to be precisely at the Fermi-energy and in the whole frequency range the density of states has to exactly have a power law dependence on frequency in order to give rise to a pair susceptibility that is subject to a perfect energy-temperature scaling. By detuning the vHS away from the Fermi energy, or incorporating another scale even at the boundary of the measured frequency range, this scaling is lost.

MFL and MFL+vHS pair susceptibilities

In real frequency, the imaginary part of the MFL self energy is of the form

$$\Sigma(\omega) = -a\pi \begin{cases} \max\{|\omega|, T\}, & \text{for } \omega < \omega_E \\ \omega_E, & \text{for } \omega > \omega_E. \end{cases} \quad (\text{B1})$$

From the spectral representation,

$$\Sigma(i\omega_n) = \frac{1}{\pi} \int_{-\infty}^{\infty} d\nu \frac{\Sigma''(\nu)}{\nu - i\omega_n}, \quad (\text{B2})$$

we obtain the self energy in imaginary frequency

$$\Sigma(i\omega_n) = -a\omega_n \left(\frac{2T}{\omega_n} \arctan \frac{T}{\omega_n} - \frac{2\omega_E}{\omega_n} \arctan \frac{T}{\omega_n} + \pi \frac{\omega_E}{|\omega_n|} + \log \frac{\omega_n^2 + \omega_E^2}{\omega_n^2 + T^2} \right). \quad (\text{B3})$$

Consider first the case where the DOS is a constant of energy. We calculate $\chi''(\omega, T)$ with both a smooth BCS type pairing glue (MFLBCS) and a quantum critical glue (MFLCG). The results are plotted in Fig. 8, from which we see no energy-temperature scaling for either of the two models. In addition, one can check that at large temperatures for MFLBCS, χ'' goes over to the BCS tanh form. The pair susceptibility is thus still marginal in this sense. The inclusion of a nontrivial self energy destroys the “marginal” scaling behavior of FLBCS. For MFLCG, the effects of the glue interactions are so strong that one ends up with a result that is barely distinguishable from CGBCS.

To our knowledge, the only way that the pair susceptibility of a MFL can resemble that of QCBSC/HSAdS₂ in some sense is to invoke a van Hove singularity in the spectrum. The idea that the presence of vHS in the DOS is responsible for high temperature superconductivity has been around for some time (see^{53–56} and references therein). An extended van Hove singularity right at the Fermi level can produce a relevant pair susceptibility, i.e. the real part of the pair susceptibility $\chi'(\omega = 0, T)$ has an algebraic temperature dependence.²⁹ But as will be shown below, extreme fine-tuning is needed to get energy-temperature scaling for the imaginary part of the pair susceptibility. Moreover, although there are indications of the presence of extended vHS in cuprates,^{30,31} to the best of our knowledge they have not been found in typical heavy fermion materials.

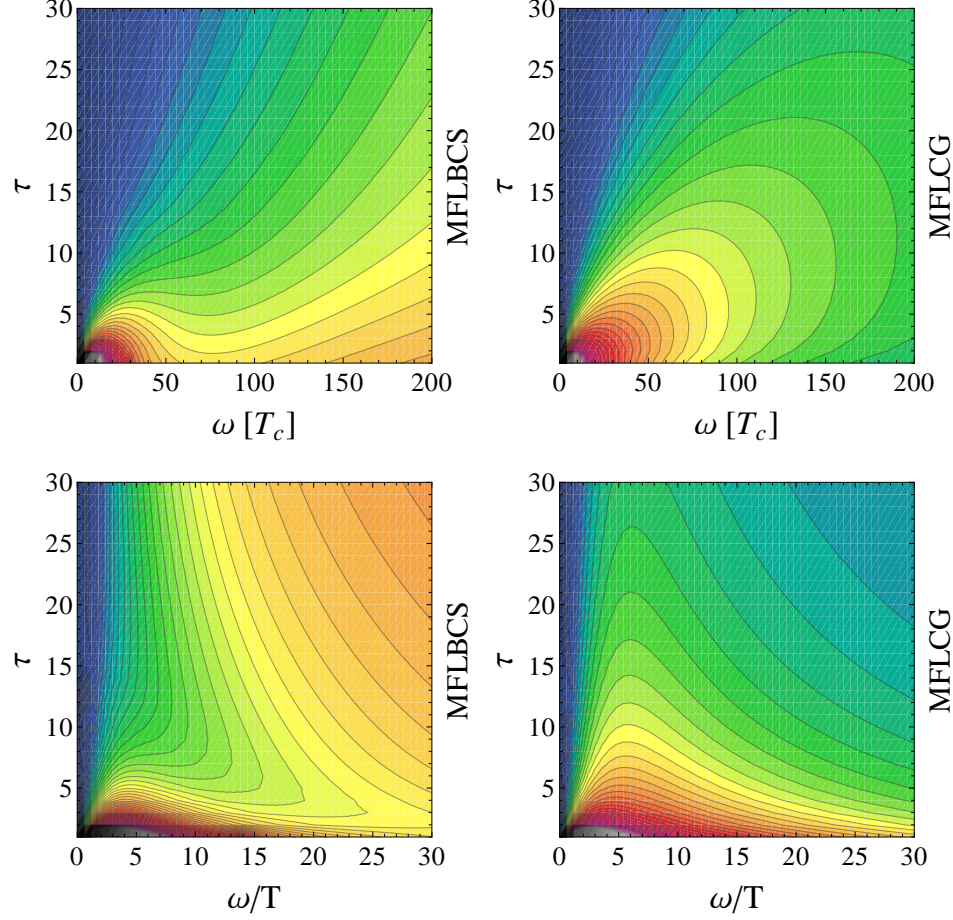


FIG. 8: (Color online) **Marginal Fermi liquid pair susceptibility with smooth density of states.** *Top:* False-color plot of the imaginary part of the pair susceptibility χ'' as function of frequency ω (in units of T_c) and reduced temperature $\tau = (T - T_c)/T_c$, for two different models: marginal Fermi-liquid with BCS pairing and marginal Fermi-liquid with critical glue. In both cases, the density of states is taken to be constant. *Bottom:* the same plot, but now the horizontal axis is rescaled by temperature while the magnitude is rescaled by temperature to a certain power: we are plotting $T^\delta \chi''(\omega/T, \tau)$, in order to show energy-temperature scaling at high temperatures. Here for both models $T_c = 0.01$ and $\delta = 0$. The color scheme is the same as used in the main text. For MFLBCS, the parameters are $a = 0.3, \omega_E = 1, g = 0.9627, \omega_b = 0.5$. For MFLCG, we take $a = 0.4, \omega_E = 0.2, \gamma = 1/3, \Omega_0 = 0.0134$.

With the inclusion of a nontrivial DOS $N(\epsilon)$, the electronic vertex operator becomes

$$\Gamma_0(i\nu_n, i\Omega) = \frac{T}{N_0} \int_{-\infty}^{\infty} d\epsilon N(\epsilon) \frac{1}{-i\nu_n - \epsilon - \Sigma(-i\nu_n)} \frac{1}{i\nu_n + i\Omega - \epsilon - \Sigma(i\nu_n + i\Omega)}. \quad (\text{B4})$$

For MFL, $\chi''(\omega, T)$ can only be calculated numerically. But the basic picture can be illustrated by considering the non-interacting limit, where one has simply $\chi''_0(\omega) = N(\omega/2) \tanh(\omega/4T)$. In this case, one can easily see that, to get energy-temperature scaling for χ'' , i.e. $\chi''(\omega, T) \rightarrow T^\delta \mathcal{F}(\omega/T)$, the DOS has to be a power of energy in the whole frequency range that is experimentally relevant, $N(\epsilon) = |\epsilon|^{-\alpha}$. Any deviation from this special form will break energy-temperature scaling. This can be illustrated by considering several explicitly deformations from the strict power form of the DOS.

One example is that the van Hove singularity moves away from the Fermi level (vH1MFLBCS). Consider DOS of the form $N(\epsilon) = |\epsilon + \mu|^{-1/2}$, we obtain the electronic vertex operator

$$\Gamma_0(i\nu_n, i\Omega) = \frac{-\pi T}{N_0(i\Omega_+ - i\Omega_-)} \left(\frac{1}{\sqrt{i\Omega_+ + \mu}} - \frac{1}{\sqrt{-i\Omega_+}} \frac{1}{\sqrt{1 - i\mu/\Omega_+}} - \frac{1}{\sqrt{i\Omega_- + \mu}} + \frac{1}{\sqrt{-i\Omega_-}} \frac{1}{\sqrt{1 - i\mu/\Omega_-}} \right), \quad (\text{B5})$$

with $i\Omega_+ \equiv i\nu_n + \Omega - \Sigma(i\nu_n + i\Omega)$ and $i\Omega_- \equiv -i\nu_n - \Sigma(-i\nu_n)$. Another example is where there is an extra exponential

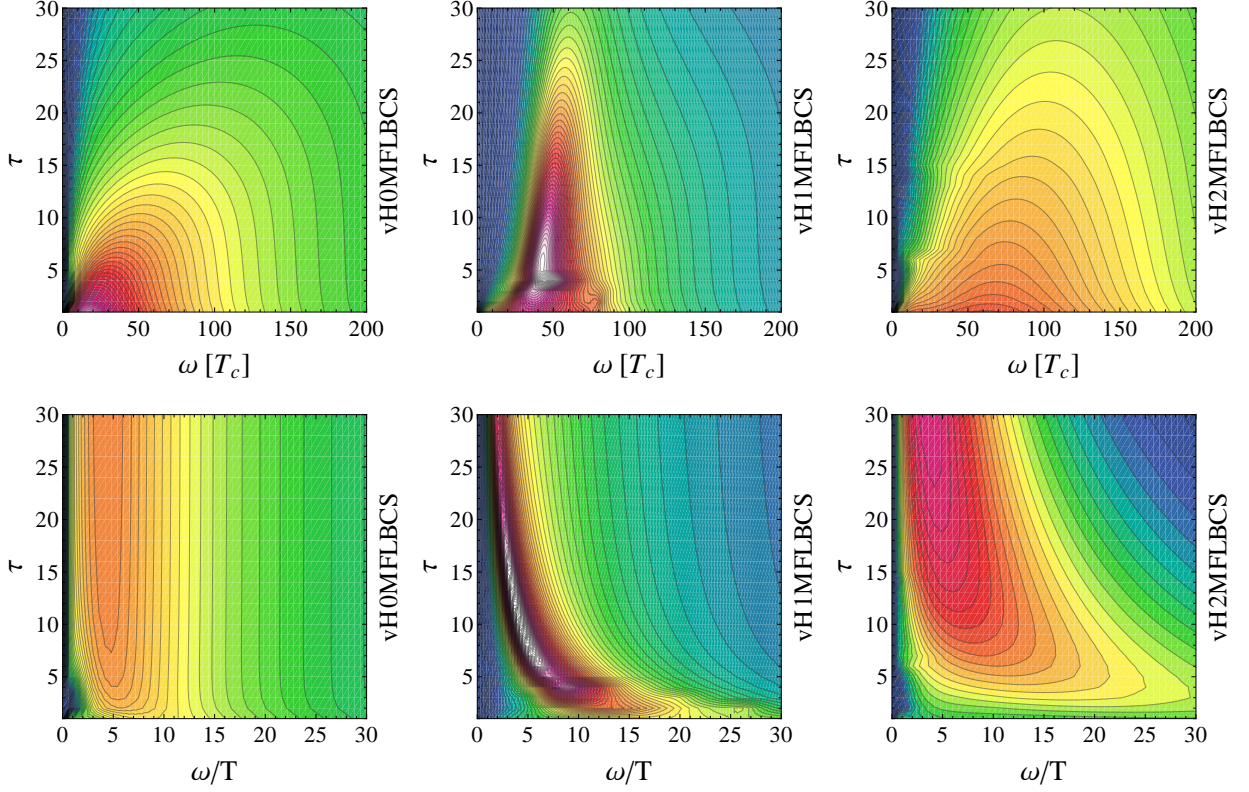


FIG. 9: (Color online) **Marginal Fermi liquid pair susceptibility with van Hove singularities.** The same plot as Fig. 8 for marginal Fermi-liquid with extended van Hove singularities. The pairing interactions are all of the BCS type. The density of states is $N(\epsilon) = |\epsilon|^{-1/2}, |\epsilon + \mu|^{-1/2}, |\epsilon|^{-1/2} \exp(-|\epsilon|/\omega_d)$ for the three different cases respectively. Here $T_c = 0.01$, and the scaling exponent $\delta = 1/2$ for all three models. For vH0MFLBCS, the parameters are $a = 0.1445, \omega_E = 0.05, g = 0.2, \omega_b = 0.05$. For vH1MFLBCS, we take $\mu = -0.25, a = 0.2, \omega_E = 0.05, g = 0.5634, \omega_b = 0.05$. For vH2MFLBCS, the parameters are $\omega_d = 2, a = 0.3, \omega_E = 0.4, g = 0.3178, \omega_b = 0.1$.

suppression of DOS at large energies (vH2MFLBCS), i.e. $N(\epsilon) = |\epsilon|^{-1/2} \exp(-|\epsilon|/\omega_d)$, for which one has

$$\Gamma_0(i\nu_n, i\Omega) = \frac{-\pi T}{N_0(i\Omega_+ - i\Omega_-)} (F(\Omega_+) - F(-\Omega_+) - F(\Omega_-) + F(-\Omega_-)), \quad (\text{B6})$$

with $F(\Omega) = (i\Omega)^{-1/2} \exp(i\Omega/\omega_d) \text{Erfc}[(i\Omega/\omega_d)^{1/2}]$. The results are plotted in Fig. 9 together with the case where the DOS is of the strict power law form (vH0MFLBCS). One can see that energy-temperature scaling is broken for the two deformed cases.

Further comments on the relation between MFL and QCBCS/HS

The QCBCS/HS approach is not really in conflict with MFL, which is well-known to be able to capture a large amount of experimental results in cuprates and heavy fermions. The pursuit of QCBCS/HS is actually orthogonal to that of MFL. MFL attacks the single particle Green's functions, while QCBCS/HS focuses on the particle-particle channel. Due to vertex corrections, the two channels are not necessarily simply related. A clear illustration of this is the Luttinger liquid, where these two channels have separate energy-temperature scaling with distinctive exponents. AdS/CFT seems to provide a natural framework to incorporate such Luttinger-liquid-type scaling behavior in high dimensional systems, going well beyond a Hertz-Millis type interpretation of MFL. Probing the AdS_2 background with fermions, one obtains the MFL type behavior in the fermion Green's functions; by probing the AdS_2 background with bosonic order parameters, one can detect energy-temperature scaling in the corresponding susceptibility. If we take MFL as synonymous to the fact that the electron scattering rate is proportional to the larger of temperature or frequency, the contest, that the pair tunneling experiment proposed in this paper is trying to settle, is really between

the Hertz-Millis type interpretation of MFL and the holographic (or call it the Luttinger-liquid-type) interpretation of MFL.

-
- ¹ M. R. Norman, *Science* **332**, 196 (2011).
 - ² J. Zaanen, in *100 years of superconductivity* (eds Rogalla, H. & Kes, P. H.) (Taylor & Francis, 2011, in press). Preprint at <http://arxiv.org/abs/1012.5461v2> (2010).
 - ³ F. Wang and D.-H. Lee, *Science* **332**, 200 (2011).
 - ⁴ C. Pfleiderer, *Rev. Mod. Phys.* **81**, 1551 (2009).
 - ⁵ S. Sachdev, *Quantum Phase Transitions* (Cambridge Univ. Press, New York, 1999).
 - ⁶ H. v. Löhneysen, A. Rosch, M. Vojta and P. Wölfle, *Rev. Mod. Phys.* **79**, 1015 (2007).
 - ⁷ P. Gegenwart, Q. Si, and F. Steglich, *Nature Physics* **4**, 186 (2008).
 - ⁸ S. Sachdev, and B. Keimer, *Physics Today* **64**, 29 (2011).
 - ⁹ E.-G. Moon and A. V. Chubukov, *J. Low Temp. Phys.* **161**, 263 (2010). and references therein.
 - ¹⁰ J. She and J. Zaanen, *Phys. Rev. B* **80**, 184518 (2009).
 - ¹¹ S. A. Hartnoll, C. P. Herzog and G. T. Horowitz, *Phys. Rev. Lett.* **101**, 031601 (2008).
 - ¹² T. Faulkner, G. T. Horowitz and M. M. Roberts, *JHEP* **04**, 051 (2011).
 - ¹³ R. A. Ferrell, *J. Low Temp. Phys.* **1**, 423 (1969).
 - ¹⁴ D. J. Scalapino, *Phys. Rev. Lett.* **24**, 1052 (1970).
 - ¹⁵ J. T. Anderson and A. M. Goldman, *Phys. Rev. Lett.* **25**, 743 (1970).
 - ¹⁶ A. M. Goldman, *J. Supercond. Nov. Magn.* **19**, 317 (2006).
 - ¹⁷ N. Bergeal *et al.*, *Nature Physics* **4**, 608 (2008).
 - ¹⁸ B. Jankó, I. Kosztin, K. Levin, M. R. Norman and D. J. Scalapino, *Phys. Rev. Lett.* **82**, 4304 (1999).
 - ¹⁹ W. L. McMillan and J. M. Rowell in *Superconductivity*, Vol. 1 (ed. Parks, R. D.) (Dekker, 1969).
 - ²⁰ D. J. Scalapino, in *Superconductivity*, Vol. 1 (ed. Parks, R. D.) (Dekker, 1969).
 - ²¹ J. P. Carbotte, *Rev. Mod. Phys.* **62**, 1027 (1990).
 - ²² P. Monthoux, D. Pines and G. G. Lonzarich, *Nature* **450**, 1177 (2007).
 - ²³ D. J. Scalapino, *Physica. C* **470**, S1 (2010).
 - ²⁴ J. A. Hertz, *Phys. Rev. B* **14**, 1165 (1976).
 - ²⁵ A. V. Chubukov, D. Pines and J. Schmalian, in *The physics of superconductors*, Vol. 1 (eds Bennemann, K. H. & Ketterson, J. B.) (Springer, 2004).
 - ²⁶ A. V. Chubukov and J. Schmalian, *Phys. Rev. B* **72**, 174520 (2005).
 - ²⁷ A. Abanov, A. V. Chubukov and J. Schmalian, *Adv. Phys.* **52**, 119 (2003).
 - ²⁸ S.-X. Yang, *et al.*, *Phys. Rev. Lett.* **106**, 047004 (2011).
 - ²⁹ K.-S. Chen, *et al.*, Preprint at <http://arxiv.org/abs/1104.3261v2> (2011).
 - ³⁰ D. S. Dessau, *et al.*, *Phys. Rev. Lett.* **71**, 2781 (1993).
 - ³¹ K. Gofron, *et al.*, *Phys. Rev. Lett.* **73**, 3302 (1994).
 - ³² A. Piriou, *et al.*, *Nature Communications* **2**, 221 (2011).
 - ³³ J. Maldacena, *Adv. Theor. Math. Phys.* **2**, 231 (1998).
 - ³⁴ S. S. Gubser, I. R. Klebanov and A. M. Polyakov, *Phys. Lett. B* **428**, 105 (1998).
 - ³⁵ E. Witten, *Adv. Theor. Math. Phys.* **2**, 253 (1998).
 - ³⁶ S. A. Hartnoll, C. P. Herzog and G. T. Horowitz, *JHEP* **12**, 015 (2008).
 - ³⁷ G. E. Blonder, M. Tinkham and T. M. Klapwijk, *Phys. Rev. B* **25**, 4515–4532 (1982).
 - ³⁸ S. Kambe, H. Sakai, Y. Tokunaga and R. E. Walstedt, *Phys. Rev. B* **82**, 144503 (2010).
 - ³⁹ Y. Matsumoto, *et al.*, *Science* **331**, 316 (2011).
 - ⁴⁰ H. Shishido, *et al.*, *Science* **327**, 980–983 (2010).
 - ⁴¹ O. Fischer, M. Kugler, I. Maggio-Aprile, C. Berthod and C. Renner, *Rev. Mod. Phys.* **79**, 353–419 (2007).
 - ⁴² W. K. Park, J. L. Sarrao, J. D. Thompson and L. H. Greene, *Phys. Rev. Lett.* **100**, 177001 (2008).
 - ⁴³ Y. Noat, *et al.*, *J. Phys. Condens. Matter* **22**, 465701 (2010).
 - ⁴⁴ G. A. Baker and P. Graves Morris, *Padé approximants* (Addison-Wesley, Reading, 1981).
 - ⁴⁵ H. J. Vidberg and J. W. Serene, *J. Low Temp. Phys.* **29**, 179–192 (1977).
 - ⁴⁶ K. S. D. Beach, R. J. Gooding and F. Marsiglio, *Phys. Rev. B* **61**, 5147–5157 (2000).
 - ⁴⁷ S. S. Gubser, *Phys. Rev. D* **78**, 065034 (2008).
 - ⁴⁸ D. T. Son and A. O. Starinets, *JHEP* **0209**, 042 (2002).
 - ⁴⁹ I. R. Klebanov and E. Witten, *Nucl. Phys. B* **556**, 89 (1999).
 - ⁵⁰ T. Faulkner, H. Liu, J. McGreevy and D. Vegh, Preprint at <http://arxiv.org/abs/0907.2694v1> (2009).
 - ⁵¹ E. Witten, Preprint at <http://arxiv.org/abs/hep-th/0112258v3> (2001).
 - ⁵² T. Faulkner, N. Iqbal, H. Liu, J. McGreevy and D. Vegh, *Science* **329**, 1043 (2010).
 - ⁵³ J. Friedel, *J. Phys.: Condens. Matter* **1**, 7757 (1989).
 - ⁵⁴ R. S. Markiewicz, *International Journal of Modern Physics B* **5**, 2037 (1991).
 - ⁵⁵ D. M. Newns, H. R. Krishnamurthy, P. C. Pattnaik, C. C. Tsuei and C. L. Kane, *Phys. Rev. Lett.* **69**, 1264 (1992).

⁵⁶ A. A. Abrikosov, J. C. Campuzano and K. Gofron, *Physica C: Superconductivity* **214**, 73 (1993).

⁵⁷ One can lower T_c by lowering the charge of the order-parameter. Curiously the holographic theory even develops a Bose-condensate of a neutral order-parameter in the presence of a $U(1)$ chemical potential. Technically it remains difficult in this set-up to cleanly extract the AdS_2 scaling. We have, however, kept the nomenclature of “small charge” superconductor indicating that $T_c \ll \mu$.